

# Artigos científicos da SMPTE na Revista da SET

Nesta edição da Revista da SET voltamos a publicar alguns dos principais artigos da *Society of Motion Picture and Television Engineers* (SMPTE), entidade que sempre trouxe credibilidade e seriedade para a indústria de radiodifusão - sobretudo, quando falamos de trabalhos técnicos e científicos e, principalmente, de normatização e padronização. É ao SMPTE que devemos creditar muitas das iniciativas que renderam inovações em todos os setores da indústria *broadcast*, desde as tecnologias de filmagem e de captação, até a edição e a transmissão de conteúdos. A SET tem muito orgulho de firmar mais esta parceria e trazer à seus associados e leitores da Revista da SET este tão prestigiado conteúdo. Esta ação faz parte do contínuo esforço que a Sociedade Brasileira de Engenharia de Televisão tem feito para posicionar nosso mercado em um patamar global. É, também, um esforço de aprimoramento de todos os nossos produtos editoriais e científicos, levando em conta as necessidades dos profissionais que fazem parte de nosso mercado. Para começar esta edição, trazemos um artigo que aborda um dos principais avanços da atualidade com a produção em Ultra Alta Definição. O primeiro estudo, produzido por destacados engenheiros japoneses, aborda o gerenciamento de cor para a produção UHDTV com destaque para o *Wide-Color-Gamut*. Os principais pontos do artigo são: Rec. 2020, Rec. 709, colorimétrica, e gerenciamento de cor.

Boa leitura!

Olímpio José Franco  
Presidente da SET

## Color Management for Wide-Color-Gamut UHDTV Production

by Kenichiro Masaoka, Takayuki Yamashita, Yukihiro Nishida, and Masayuki Sugawara

**U**ltrahigh-definition television (UHDTV) is a wide-color-gamut system, as standardized in Rec. ITU-R BT. 2020 and SMPTE ST 2036-1, that covers most real object colors and encompasses the gamuts of high-definition television (HDTV), Adobe RGB, and Digital Cinema Initiative Primary 3 (DCI-P3). The development of wide-gamut displays and high-quality gamut mapping is a major challenge in the workflow of UHDTV production today. While monochromatic light sources, such as lasers, are ideal for UHDTV wide-gamut displays, wide-gamut

liquid crystal displays with nonmonochromatic backlight sources, such as quantum dot light-emitting diodes, may well be used from the viewpoint of both cost and performance. Furthermore, a high-quality gamut mapping algorithm between UHDTV and HDTV for live broadcast production is essential. This paper offers solutions to these challenges.

**Keywords:** UHDTV, Rec. 2020, Rec. 709, colorimetry, color management, gamut mapping



## INTRODUCTION

Ultrahigh-definition television (UHDTV) is a next-generation television system that provides a better viewing experience than the popular high-definition television (HDTV) system. In August 2012, the ITU-R issued Rec. BT.2020 (Rec. 2020)<sup>1</sup> specifying the video parameter values for UHDTV production and international program exchange. The important features of Rec. 2020 include a wider color gamut than that of HDTV, as specified in Recommendation ITU-R BT.709 (Rec. 709)<sup>2</sup> in addition to the high pixel count of UHDTV1, or 4K (3840 x 2160 pixels), and UHDTV2, or 8K (7680 x 4320 pixels); a higher frame frequency of 120 Hz; and a higher bit depth of 12 bits.

Proper implementation and color management for Rec. 2020 are urgently needed for improving the effectiveness of the wide-gamut system colorimetry. **Figure 1** shows a color management workflow based on and modified from SMPTE report of the UHDTV Ecosystem Study Group.<sup>3</sup> The workflow is a type of a Rec. 2020 island in which cameras, reference displays, and waveform monitors are dedicated to UHDTV production in Rec. 2020 red, green, and blue (RGB)/Y<sub>C</sub>C<sub>R</sub> signals.

This paper introduces implementation concepts and developments of cameras and displays for Rec. 2020 colorimetry, gamut monitoring equipment, and a colorimetry converter between Rec. 2020 and Rec. 709.

## DESIGN OF UHDTV SYSTEM COLORIMETRY

The wide-gamut system colorimetry was designed based on the requirements of color encoding efficiency, program quality management, target color gamut, and efficient gamut mapping.<sup>4</sup> Considering the color encoding efficiency and program quality management, physically realizable, highly saturated RGB primaries were selected instead of additional primaries or unreal primaries. Program quality management requires that each color can be reproduced on a reference display so that broadcasters can monitor and control the color reproduction. To handle the maximum color gamut and fulfill the requirements, monochromatic RGB primaries were chosen in Rec. 2020.<sup>5,6</sup>

Primary	Chromaticity Coordinates (CIE 1931)		Corresponding Wavelength (Illuminant)
	x	y	
R	0.708	0.292	630 nm
G	0.170	0.797	532 nm
B	0.131	0.046	467 nm
Reference white	0.3127	0.3290	(D65)

**Table 1 Chromaticity coordinates of Rec. 2020 RGB primaries and the corresponding wavelengths of monochromatic light**

**Table 1** lists the chromaticity coordinates of the RGB primaries specified in Rec. 2020 and the corresponding wavelengths of monochromatic light. Rec. 2020 covers most real object colors and encompasses the gamuts of the major standard system colorimetries: Rec. 709 (for HDTV), Adobe RGB<sup>7</sup> (as a de facto standard in professional color processing), SMPTE Recommended Practice 431-2:2011<sup>8</sup> (for the reference digital cinema projector, also known as Digital Cinema Initiative Primary 3, or DCI-P3). **Figure 2** shows the chromaticities of the RGB primary sets and Pointer's colors<sup>9</sup> (representing the maximum gamut of real object colors under illuminant C) transformed to those under illuminant D65 with the CAT02 chromatic adaptation transform.<sup>10</sup> The volume coverage of Pointer's gamut by Rec. 2020 is more than 99.9% in the CIE L\*a\*b\* (CIELAB) color space.<sup>4</sup>

## CAMERA FOR REC. 2020

The spectral sensitivity properties of broadcast cameras are designed primarily based on the ideal camera spectral sensitivities.<sup>11</sup> The curves are calculated from the CIE color-matching functions by a linear transform determined by the chromaticities of the three primaries and the reference white. A color camera with the ideal spectral sensitivity curves outputs the relative amounts of the RGB primaries so that the chromaticities and relative luminances of the displayed and the original colors become identical.

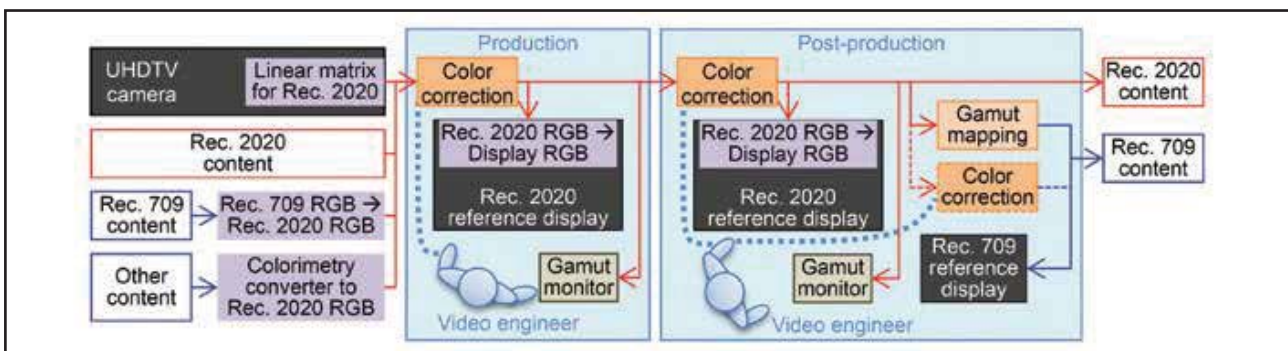


**Figure 1 UHDTV color management workflow**

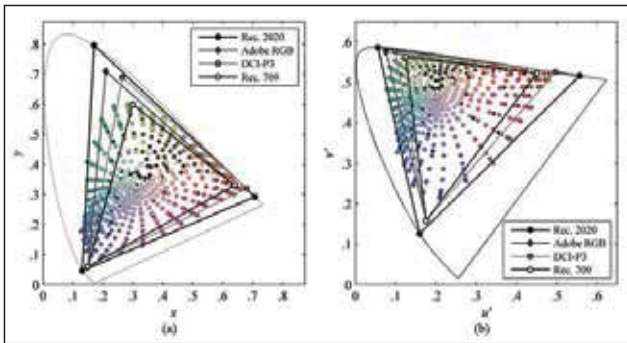


**Figure 2** Chromaticities of the RGB primary sets of the standard system colorimetries for Rec. 709, Adobe RGB, DCI-P3, and those of Pointer’s colors under illuminant D65: (a) the CIE 1931 (x, y) chromaticity diagram; (b) the CIE 1976 (u', v') chromaticity diagram

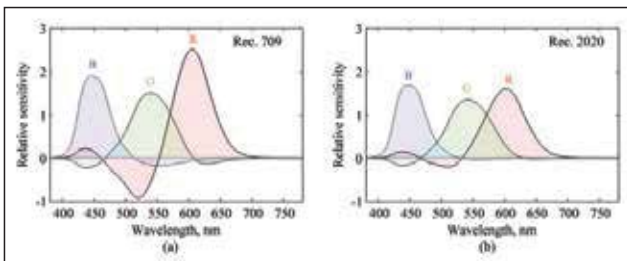


**Figure 3** Ideal camera spectral sensitivity curves: (a) Rec. 709; (b) Rec. 2020

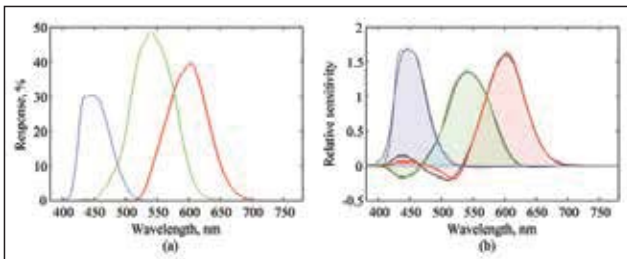


**Figure 4** Measured camera spectral response with the prism designed for Rec. 2020: (a) curves before applying the linear matrix; (b) curves obtained by applying the optimized linear matrix, superimposed on the ideal spectral sensitivity curves for Rec. 2020 shown in Fig. 3 (b)

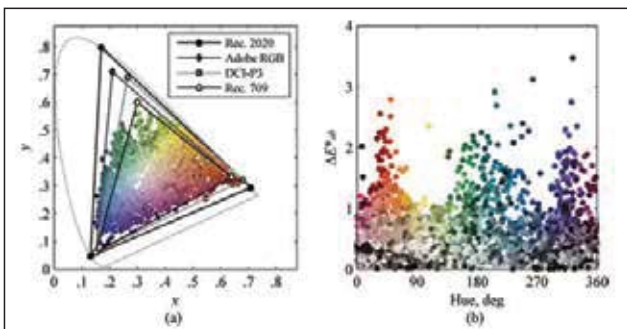


**Figure 5** (a) Chromaticity distribution of the SOCS colors in the categories of paint (not for art), paints (for art), textile, flowers, leaves, human skin, and Krinov data; (b) color errors reproduced with the optimized camera spectral sensitivity curves shown in Fig. 4 (b)

**Figure 3** shows the ideal camera spectral sensitivity curves for Rec. 709 and Rec. 2020. The theoretical ideal sensitivity curves are not physically realizable because of their negative sensitivity values. Modern cameras apply a  $3 \times 3$  matrix to the RGB linear output from their sensors with positive sensitivities to approximate the ideal spectral sensitivity as well as possible. The linear matrix correction is processed inside the camera. As **Fig. 3 (a)** shows, the negative lobes for Rec. 709 are large, which results in large negative coefficients of the off-diagonal elements of the linear matrix and degradation in the signal-to-noise ratio.

New prisms were developed and installed in our 8K video cameras.<sup>12,13</sup> **Figure 4 (a)** shows the overall spectral response, including the characteristics of the lens, prism, and sensors.<sup>5</sup> **Figure 4 (b)** shows the curves resulting from the application of an optimized linear matrix, with an average CIELAB color difference  $\Delta E_{ab}$  of 0.5 for the ColorChecker colors. For further analysis of the accuracy of the color reproduction, we used the Standard Object Colour Spectra (SOCS) database.<sup>14</sup> The spectral reflectance data was chosen in seven categories—paint (not for art), paints (for art), textile, flowers, leaves, human skin, and Krinov data—which, supposedly, are often reproduced in television programs. **Figure 5** shows the chromaticities of the colors and reproduced color errors simulated under illuminant D65. The average  $\Delta E_{ab}$  is 0.5.

**DISPLAY FOR REC. 2020**

**Laser Projector**

The colors in the Rec. 2020 gamut are preferably monitored at every stage of the workflow. Monochromatic light sources such as lasers are required for a display to fulfill the Rec. 2020 colorimetry specification. We developed an 8K laser projector<sup>15</sup> and demonstrated the effectiveness of the wide-gamut system colorimetry at the Japan Broadcasting Corporation (NHK) Science & Technology Research Laboratories (STRL) Open House in 2013.<sup>16</sup> **Figure 6** shows a photograph of the demonstration. On the left side, we placed objects with highly saturated colors. The objects were shot with the wide-gamut 8K video camera<sup>12</sup> with the new prism, and the images were displayed on the screen on the right side using the projector. The images reproduced with Rec. 2020 colorimetry were compared to those reproduced with Rec. 709 colorimetry. Every visitor easily distinguished the difference between the Rec. 709 and the Rec. 2020 images and reported that the Rec. 2020 images showed significantly greater similarity to the real objects.

**Direct-View Display with a Nonmonochromatic Light Source**

The development of direct-view wide-gamut displays is a major challenge. While liquid crystal displays (LCDs) are considered promising as UHDTV displays and laser-



**Figure 6** Demonstration of the UHDTV wide-gamut system colorimetry using the UHDTV2 video camera<sup>12</sup> with the new prism and the UHDTV2 laser projector<sup>15</sup> at the NHK STRL Open House in 2013

backlit LCDs are expected to be available in the near future, nonmonochromatic light sources may well be used from the viewpoint of both cost and performance.

It is important to provide a guideline for designing displays with nonmonochromatic light sources for Rec. 2020 and conversion methods from Rec. 2020 RGB to the displays' native RGB. The key aspects are the spectral bandwidths and peak emission wavelengths.

The quantum dot light-emitting diode (QD-LED) is emerging as a next-generation LCD backlight source for wide-gamut LCDs.<sup>17</sup> The available red and green quantum dots in QD-LEDs have approximately Gaussian emission spectra at 30 nm full width at half maximum (FWHM) when pumped by blue LEDs at 20 nm FWHM.<sup>18</sup>

Their central wavelengths are precisely tunable. We calculated the chromaticities of nonmonochromatic light sources with Gaussian emission spectra.<sup>19</sup> **Figure 7 (a)** indicates the chromaticities of the constant FWHM loci at 10, 20, ..., 110 nm FWHM meshed with the constant central wavelength loci at intervals of 5 nm and the CIELAB constant hue loci of Rec. 2020 primaries. **Figure 7 (b)-(d)** show magnified sections of **Fig. 7 (a)** around the green, blue, and red primaries, respectively. In **Fig. 7 (b)**, it can be observed that the green primaries of Adobe RGB and DCI-P3 are close to the locus at 50 nm FWHM and that the green primary of Adobe RGB is close to the constant hue locus of Rec. 2020 green primary. **Figure 7 (c)** indicates that the blue primary of Rec. 709 (the same as those of Adobe RGB and DCI-P3) lies near

the locus at 110 nm FWHM. In **Fig. 7 (d)**, the loci at different FWHMs merge to the spectral locus around red. For Rec. 2020 colorimetry, it would be preferable if the chromaticities of the primaries lie on the constant hue loci of the Rec. 2020 primaries from the viewpoints of

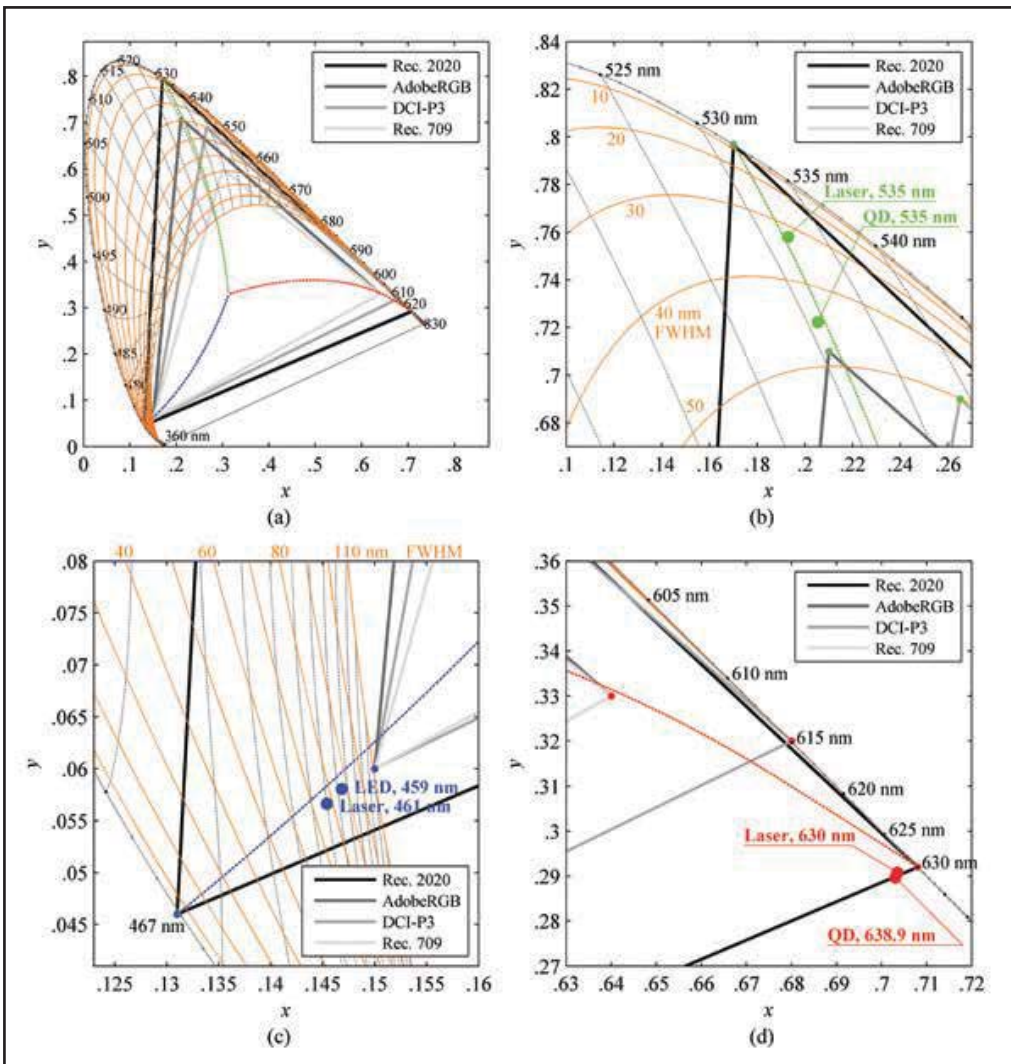


**Figure 7 (a)** Constant FWHM loci at 10, 20, ..., 110 nm FWHM meshed with constant central wavelength loci at intervals of 5 nm of Gaussian emission spectra and the CIELAB constant hue loci of Rec. 2020 primaries; (b)-(d) magnified sections around the green, blue, and red primaries with the chromaticities of the selected green, blue, and red light sources, respectively, with color filters

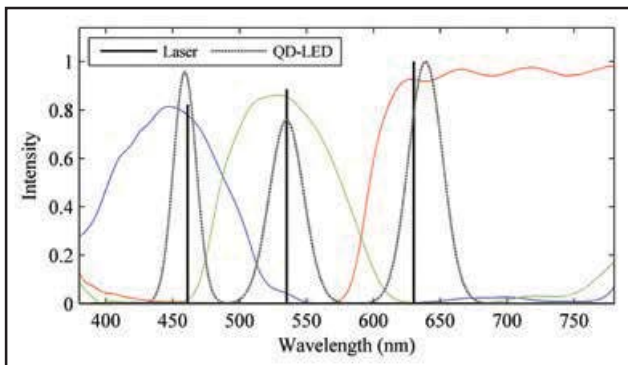


**Figure 8** Transmission spectra of color filters<sup>18</sup> and normalized spectra of the optimized laser light sources (461, 535, and 630 nm) and QD-LED light sources (459, 535, and 638.9 nm)

the gamut mapping and the coverage balance of the Rec. 2020 color gamut in terms of hue.

If ideal color filters with no crosstalk are used for LCDs, the chromaticities of the RGB primaries are determined by their central wavelengths and FWHMs. However, the current color filters used in LCDs are not ideal. Even if sharp emission spectra of light sources are realized, the color-filter crosstalk can reduce the purity of the RGB primaries. **Figure 8** shows the transmission spectra of the nonideal color filters, as provided by Luo *et al.*<sup>18</sup> We simulated the chromaticities of two sets of RGB light sources with color filters: one for monochromatic light sources and the other for nonmonochromatic QD-LED light sources. When the wavelengths of the light sources are optimized for the nonideal color filters so that the chromaticities of the primaries lie close to the constant hue loci of Rec. 2020 primaries, as shown in **Fig. 7 (b)-(d)**, it is observed that the purity of the RGB primaries is significantly reduced even when using monochromatic light sources with the optimized wavelengths. It is therefore necessary to optimize color filters for Rec. 2020 colorimetry for both monochromatic and nonmonochromatic light sources. We are developing wide-gamut LCDs for UHDTV using new color filters optimized for Rec. 2020.

**MONITORING REC. 2020 GAMUT**

For now, we assume that reference displays with nonmonochromatic light sources are likely to be used. When using such a display, the input Rec. 2020 RGB values are transformed to the display’s native RGB values by a 3 x 3 matrix multiplication and then clipped to the range’s extremes. This transform should be applied to monitoring only, not for processing of the main signal. Reference displays that do not achieve the Rec. 2020 gamut must reproduce the widest possible color gamut according to guidelines yet to be developed. It will be helpful for video engineers when the colors outside the gamut of the reference displays are highlighted



**Figure 9** Waveform monitor displaying the chromaticity distribution of the input video signal

on the screens or other monitoring equipment. We have developed a waveform monitor for Rec. 2020 colorimetry, shown in **Fig. 9**, that can display the chromaticity distribution of the input content on the xy or u’v’ chromaticity diagram in realtime.

**COLORIMETRY CONVERSION BETWEEN REC. 2020 AND REC. 709**

In the wide-gamut UHDTV workflow, we must transform colors across color spaces with different color gamuts. For the input content, several non-Rec. 2020 colorimetries are likely to be used, and their gamuts may be smaller than the Rec. 2020 gamut. In these cases, the colors must be reproduced as mastered in each colorimetry. However, Rec. 2020 colors of mastered content may need to be converted to Rec. 709 colors, where gamut mapping is needed. Furthermore, a high-quality gamut mapping algorithm that can be used for live broadcast production is essential. This section introduces methods for colorimetry conversion between Rec. 2020 and Rec. 709.

**Transform from Rec. 709 to Rec. 2020**

The colors must be reproduced as mastered in Rec. 709 colorimetry without alteration. For this requirement, we propose the use of a 3 x 3 linear matrix. The nonlinear Rec. 709 RGB values are linearized by the inverse optoelectronic transfer function (OETF) and then transformed to the linear Rec. 2020 RGB values as

$$\begin{bmatrix} E_R \\ E_G \\ E_B \end{bmatrix}_{2020} = \begin{bmatrix} 0.6274 & 0.3293 & 0.0433 \\ 0.0691 & 0.9195 & 0.0114 \\ 0.0164 & 0.0880 & 0.8956 \end{bmatrix} \begin{bmatrix} E_R \\ E_G \\ E_B \end{bmatrix}_{709}$$

After the transform, the linear Rec. 2020 RGB values are nonlinearized by the OETF.

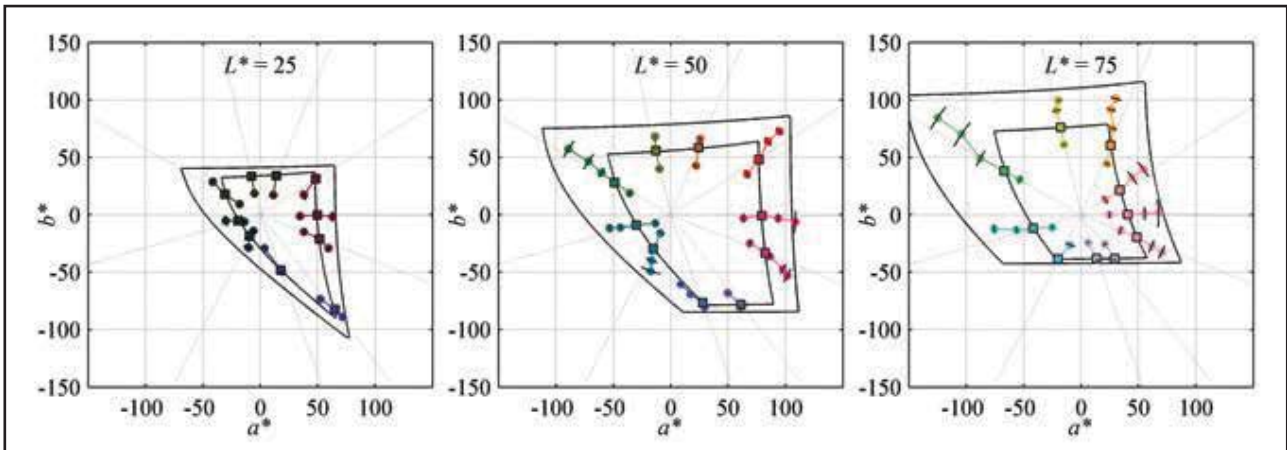


Figure 10 Mean constant perceived hues with standard deviations ( $N = 25$ ). Square markers show the reference colors

### Gamut Mapping from Rec. 2020 to Rec. 709

It is naturally assumed that Rec. 2020 UHDTV content is often downconverted to Rec. 709 HDTV content, where gamut mapping is inevitable. We set the following requirements for the gamut mapping algorithm with respect to the image quality and feasibility:

- Small perceived hue change.
- Unchanged colors inside the Rec. 709 gamut.
- No significant loss of spatial details, change of lightness and image contrast, or reduction of chroma.
- No visible discontinuity in lightness, chroma, or hue.
- Mathematically definable mapping.

In general, the operation of gamut mapping algorithms is based on establishing specific relationships between the appearance attributes of a source and those of a destination. In most cases, the intention is to keep a source's hues unchanged. The best color appearance model for gamut mapping algorithms defined in terms of an intended effect in color appearance is the one that most accurately predicts color appearance attributes.<sup>20</sup>

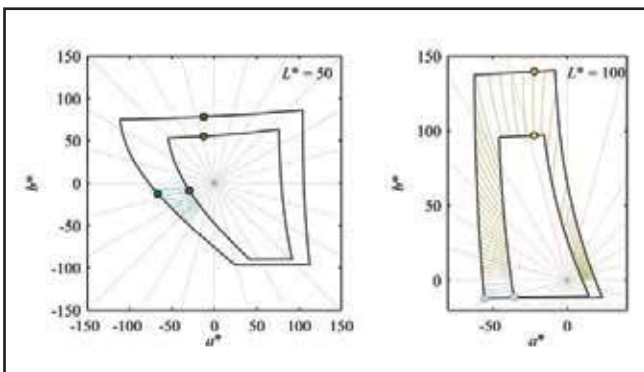


Figure 11 Rec. 2020 and Rec. 709 gamut boundaries at constant lightness sections ( $L^* = 50$  and  $100$ ) on the CIELAB  $a^*b^*$  planes. The out-of-gamut yellow highlight and cyan are mapped along the yellow and cyan loci, respectively

However, gamut mapping using the latest color appearance model, CIECAM02,<sup>10</sup> results in a significant hue discontinuity.<sup>21</sup> One reason for this is that even the latest color appearance model fails to predict the appearance attributes of saturated colors outside the psychophysical data from which it was derived.<sup>22</sup> Another reason is that designing a welltailored gamut mapping algorithm requires not only an accurate color appearance model, but also proper care of the shapes of the source and destination gamuts.

To ascertain the constant perceived hues inside the Rec. 2020 gamut, we measured them using our laser projector.<sup>23</sup> Twenty-five observers performed a matching task involving 10 hue angles at three lightness values

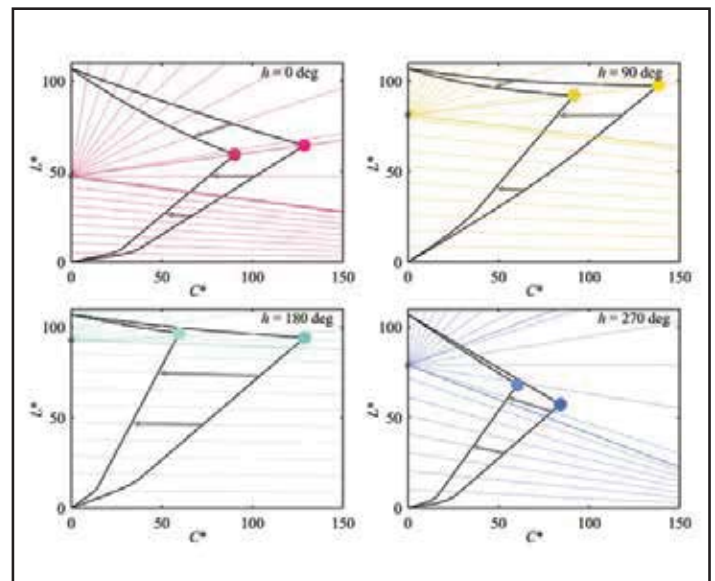


Figure 12 Rec. 2020 and Rec. 709 gamut boundaries at constant hue sections ( $h = 0^\circ, 90^\circ, 180^\circ, \text{ and } 270^\circ$ ) on the CIELAB  $C^*L^*$  planes. The colors out of the Rec. 709 gamut are mapped along the colored lines on each constant hue section



**Figure 13** Rec. 2020 images and converted ones: (a) reference; (b) proposed gamut mapping; (c) constant lightness and hue while clipping chroma in the CIELAB color space

in the CIELAB color space. **Figure 10** shows the results. Although nonlinearity of the CIELAB metric hue angle was observed in the blue region, the difference between the Rec. 2020 and the Rec. 709 gamuts in the blue region is small and the nonlinearity is negligible. However, cyan on the Rec. 709 gamut boundary consistently appeared greenish when compared to the out-of-gamut cyan with the same CIELAB metric hue angle for both color patches and natural images.

High-quality gamut mapping from Rec. 2020 to Rec. 709 requires an engineered approach to carefully handle both the Rec. 2020 and Rec. 709 irregular gamut boundaries while considering the accuracy of the color appearance model used in the gamut mapping algorithm. From an engineering viewpoint, we developed a gamut mapping algorithm from Rec. 2020 to Rec. 709 that meets the preceding requirements. The algorithm maps the out-of-gamut colors (in the region between Rec. 2020 and Rec. 709 gamut boundaries) while keeping the hue unchanged in the CIELAB color space, except for the yellow highlight and cyan. **Figure 11** shows the Rec. 2020 and Rec. 709 gamut boundaries at the constant lightness sections ( $L^* = 50$  and  $100$ ) on the CIELAB  $a^*b^*$  planes. The out-of-gamut yellow highlight and cyan are mapped along the yellow and cyan loci, respectively, indicated in **Fig. 11**. The loci deviate from the radial lines from the origin. Such deviations are applied to yellow highlight with a lightness value greater than 92.83 and a hue angle in the range of  $0^\circ$  to  $180^\circ$ , in which an excessive chroma reduction resulting in blown-out white is prevented. The mapping loci for cyan are applied to colors with any lightness values, with the hue angle ranging from  $180^\circ$  to  $240^\circ$ . **Figure 12** indicates the Rec. 2020 and Rec. 709 gamut boundaries at the constant hue sections ( $h = 0^\circ, 90^\circ, 180^\circ, \text{ and } 270^\circ$ ) on the CIELAB  $C^*L^*$  planes. The colors out of the Rec. 709 gamut are mapped onto the



**Figure 14** Realtime gamut converter with a dual-link HD-SDI input/output (1080/60/I, RGB 4:4:4, 10 bits) and a 3D lookup table of  $129 \times 129 \times 129$  grid points

Rec. 709 boundary along the colored lines indicated in **Fig. 12** on each constant hue section. The out-of-gamut colors are mapped along the lines toward a focal point on the lightness axis or along the radial lines emanating from a focal point on the chroma axis. This mapping loosens the constant lightness condition to prevent excessive chroma reduction.

**Figure 13** shows the Rec. 2020 reproduction of wide-gamut images obtained using the proposed gamut mapping algorithm in addition to a method with constant lightness and hue while clipping chroma in the CIELAB color space. No excessive chroma loss was observed in the yellow highlight, and the perceived hue of the cyan was improved in our method.

The algorithm has been implemented in a real-time gamut converter, as shown in **Fig. 14**, with a dual-link HD-SDI input/output (1080/60/I, RGB 4:4:4, 10 bits) and a 3D lookup table of  $129 \times 129 \times 129$  grid points.

### CONCLUSION

In UHDTV wide-gamut production, the color management workflow is of particular importance. We introduced our implementation concepts and developments of cameras and displays for Rec. 2020 colorimetry, gamut monitoring equipment, and gamut converter between Rec. 2020 and Rec. 709. Currently, reference displays that do not fulfill the Rec. 2020 colorimetry specification are assumed to be used in the workflow because of cost and performance considerations.

The formulation of guidelines is needed to develop widegamut displays using currently available nonmonochromatic RGB light sources. It is also an urgent requirement to optimize color filters for wide-gamut LCDs. On the basis of the set requirements for colorimetry conversion between Rec. 2020 and Rec. 709, we propose the use of a  $3 \times 3$  linear matrix for Rec. 709 to Rec. 2020 conversion and a high-quality gamut mapping algorithm for Rec. 2020 to Rec. 709 conversion. We expect that our findings will facilitate the practical realization of UHDTV wide-gamut production. ■

### References

1. ITU-R Recommendation BT.2020, "Parameter Values for Ultra-High Definition Television Systems for Production and International Programme Exchange," International Telecommunications Union, Geneva, 2012.



2. ITU-R Recommendation BT.709-5, "Parameter Values for the HDTV Standards for Production and International Programme Exchange," International Telecommunications Union, Geneva, 2002.
3. SMPTE, "UHDTV Ecosystem Study Group Report," <http://standards.smpte.org>.
4. K. Masaoka, Y. Nishida, M. Sugawara, and E. Nakasu, "Design of Primaries for a Wide-Gamut Television Colorimetry," *IEEE Trans. Broadcast*, 56(4):452-457, 2010.
5. K. Masaoka, T. Soeno, Y. Kusakabe, T. Yamashita, Y. Nishida, and M. Sugawara, "UHDTV System Colourimetry and Technical Development for Its Implementation," *ABU Technical Review*, 257:2-7, 2014.
6. ITU-R Report BT.2246-2, "The Present State of Ultra-High Definition Television," International Telecommunications Union, Geneva, 2012.
7. Adobe Systems, "Adobe RGB (1998) Color Image Encoding," San Jose, CA, May 2005.
8. SMPTE RP 431-2 (2011), "D-Cinema Quality—Reference Projector and Environment," <http://standards.smpte.org>.
9. M. R. Pointer, "The Gamut of Real Surface Colour," *Color Res. Appl.*, 5(3):145-155, 1980.
10. CIE Pub. 159, "A Colour Appearance Model for Colour Management Systems: CIECAM02," International Commission on Illumination, Vienna, 2004.
11. W. N. Sproson, *Colour Science in Television and Display Systems*, Adam Hilger: Bristol, U.K., 1983.
12. K. Masaoka, Y. Nishida, T. Soeno, T. Yamashita, M. Sugawara, and A. Saita, "Designing camera spectral sensitivities for UHDTV," *SMPTE Mot. Imag. J.*, 123(8):26-32, Nov/Dec 2014.
13. H. Shimamoto, K. Kitamura, T. Watabe, H. Ohtake, N. Egami, Y. Kusakabe, Y. Nishida, S. Kawahito, T. Kosugi, T. Watanabe, T. Yanagi, T. Yoshida, and H. Kikuchi, "120 Hz Frame-Rate Super Hi-Vision Capture and Display Devices," *SMPTE Mot. Imag. J.*, 122(2):55-61, March 2013.
14. ISO/TR 16066, "Graphic Technology—Standard Object Colour Spectra Database for Colour Reproduction Evaluation," International Organization for Standardization, Geneva, 2003.
15. Y. Kusakabe, Y. Iwasaki, and Y. Nishida, "Wide-Color-Gamut Super Hi-Vision Projector," *Proc. ITE Annual Convention*, 16-1, 2013 (in Japanese).
16. NHK, "STRL Open House 2013," [http://www.nhk.or.jp/strl/open2013/tenji/tenji20/index\\_e.html](http://www.nhk.or.jp/strl/open2013/tenji/tenji20/index_e.html).
17. Z. Luo, D. Xu, and S.-T. Wu, "Emerging Quantum-Dots-Enhanced LCDs," *J. Display Technol.* 10(7):526-539, July 2014.
18. Z. Luo, Y. Chen, and S.-T. Wu, "Wide Color Gamut LCD with a Quantum Dot Backlight," *Opt. Express*, 21(22):26,269-26,284, 2013.
19. K. Masaoka, Y. Nishida, and M. Sugawara, "Designing Display Primaries with Currently Available Light Sources for UHDTV Wide-Gamut System Colorimetry," *Opt. Express*, 22(16):19,069-19,077, 2014.
20. J. Morovic, *Color Gamut Mapping*, Wiley: New York, 2008.
21. J. Froehlich, A. Schilling, and B. Eberhardt, "Gamut Mapping for Digital Cinema," *SMPTE Mot. Imag. J.*, 123(8):41-48, Nov/Dec 2014.
22. J. Morovic, V. Cheung, and P. Morovic, "Why We Don't Know How Many Colors There Are," *Proc. 6th European Conference on Colour in Graphics, Imaging, and Vision*, pp. 49-53, 2012.
23. Y. Iwasaki, K. Masaoka, Y. Kusakabe, and Y. Nishida, "Subjective Evaluation of Constant Perceived Hue in the UHDTV Wide-Gamut," *IEICE Tech. Rep.*, 114(171):1-5, 2014 (in Japanese).

Presented at the SMPTE 2014 Annual Technical Conference & Exhibition, Hollywood, CA, 21-23 October 2014. Copyright © 2015 by SMPTE.



**Kenichiro Masaoka** received a B.S. in electronics engineering and an M.S. in energy engineering from the Tokyo Institute of Technology, Tokyo, Japan. He joined Japan Broadcasting Corp. (NHK) in 1996. He is principal research engineer for the Advanced Television Systems Research Division, NHK Science & Technology Research Laboratories (STRL), Tokyo. He received a Ph.D. in engineering from the Tokyo Institute of Technology in 2009. His research interests include color science, human vision, and digital imaging systems. He is a member of the Institute of Electrical and Electronics Engineers (IEEE), SMPTE, and the Institute of Image Information and Television Engineers of Japan (ITE).



**Takayuki Yamashita** is senior research engineer for the Advanced Television Systems Research Division of NHK Science & Technology Research Laboratories (STRL). He is working on the research of UHDTV systems and his research fields include the development of camera systems, image sensors, and high-bandwidth digital signal processing and transmission systems. He also has an interest in the research of capturing system for next-generation 3DTV. Yamashita joined NHK in 1995 after receiving B.E. and M.E. degrees in electronic engineering and information science from Kyoto Institute of Technology, Kyoto, Japan, in 1993 and 1995, respectively. He has been engaged in research of HDTV camera systems since 1999. He is a member of SMPTE and ITE and is also active in the standardization of broadcast technologies in the Association of Radio Industries and Businesses (ARIB).



**Yukihiro Nishida** is senior research engineer for the Advanced Television Systems Research Division of NHK STRL. He has been involved in many areas of broadcasting technologies, including HDTV, digital broadcasting, video coding, multiplexing, quality evaluation, and UHDTV. He is also active in the standardization of broadcast technologies in ITU-R and the ARIB. He is vice-chair of the ITU-R Study Group 6 on Broadcasting Services, and is also chair of Working Party 6B. Nishida received B.S. and M.S. degrees in electric engineering from Keio University, Yokohama, Japan, and a Ph.D. in engineering from the University of Electro-Communications, Tokyo, Japan.



**Masayuki Sugawara** received B.S. and M.S. degrees in electric communication engineering and a Ph.D. degree in electronic engineering from Tohoku University, Sendai, Japan. He joined NHK in 1983. Since 1987, he has been researching solid-state image sensor, HDTV camera, and the UHDTV system at NHK STRL. Sugawara was an associate professor at the University of Electro-Communications, Tokyo, Japan, from 2000 to 2004. He has been attending ITU-R SG6 meetings since 2004 and has been active in the working parties that address program production. Currently, he is deputy director of NHK STRL. Sugawara is a member of IEEE, SMPTE, the Institute of Electronics, Information and Communication Engineers (IEICE), and ITE.